This is the accepted manuscript made available via CHORUS. The article has been published as:

Molecular Scale Simulation of Homopolymer Wall Slip

John R. Dorgan and Nicholas A. Rorrer

Phys. Rev. Lett. **110**, 176001 — Published 23 April 2013

DOI: 10.1103/PhysRevLett.110.176001

Molecular Scale Simulation of Homopolymer Wall Slip

John R. Dorgan*, Nicholas A. Rorrer

Department of Chemical and Biological Engineering, Colorado School of Mines 1500 Illinois Street, Golden, CO, 80401

KEYWORDS: Polymer Wall Slip, Rheology, Molecular Simulation

*author to whom correspondence should be addressed; email: jdorgan@mines.edu

ABSTRACT: The first molecular scale simulation of highly entangled polydisperse homopolymers that is capable of capturing all three regions - no slip, weak slip, and strong slip - of the hydrodynamic boundary condition is presented. An on-lattice dynamic Monte Carlo technique capable of correctly capturing both unentangled and entangled polymer dynamics is used to study the molecular details of wall slip phenomena for homopolymers and energetically neutral walls. For unentangled chains (those exhibiting Rouse dynamics) weak slip is not present but evidence of strong slip is manifest at very high shear rates. For entangled chains (of sufficient length to exhibit reptation dynamics), both weak and strong slip are observed. Consistent with numerous experimental studies, disentanglement and cohesive failure occur at high shear rates. Disentanglement is clearly evidenced in a non-linear velocity profile that exhibits shear banding, in an excess of chain ends at the slip plane, and perhaps most importantly in a non-monotonic stress vs. shear rate response. The chain end density exhibits a pre-transitional periodicity prior to disentanglement. Unentangled Rouse chains do not show this pre-transitional response or a bifurcation in their stress vs. shear rate response. Finally, it is shown that when polydispersity is introduced, slip phenomena is severely reduced and the inherent constitutive bifurcation is limited to a small region. Predictions are in *post facto* agreement with many experiments, are distinct from existing results obtained using molecular dynamics simulation techniques, and shed light on fundamental mechanisms of polymer wall slip.

Wall slip of fluids under flow is an engaging topic that is still not fully resolved despite its importance in polymer processing[1-3], microfluidics[4], and superhydrophobicity[5]. In 1827 Navier[6] proposed the slip velocity, v_s, is linearly proportional to the shear rate with a proportionality constant, *b*. However, this simple postulate offered little physical understanding. Over a hundred years later Mooney[7] was the first to propose a series of equations and perform experiments that can be used to understand and observe slip. These equations demonstrated that by changing the gap width in a parallel plate rheometer, or by changing the diameter of a capillary rheometer, slip could be determined. Brochard and deGennes[8] elaborated on the shear rate dependent slip at a polymer/solid interface. They proposed that above a certain shear rate adsorbed polymer chains would experience a coil stretch phenomenon, in which polymer chains would stretch out and become unentangled with adjacent polymer chains. This model is widely discussed and generally accepted. However, a number of details remain unresolved.

Literature reviews on polymer slip [2, 3, 9, 10] discuss these phenomena as belonging to two categories: weak and strong. Weak slip implies the chain segments in contact with the wall "slide" along the wall; they undergo a preferential surface diffusion in the direction opposite to the moving wall. This is the case when polymer-wall interactions are literally weak. Entanglements with the bulk pull on the surface adsorbed chains more than the wall pulls on them so they slip relative to the wall. If the chains are instead strongly bound to the wall (for example, chemisorption), then they will not "slide" until the stress is very high[8] (high enough to break bonds in the case of chemisorption). In fact, the stress for desorption can be higher than the stress required to cause disentanglement with the bulk so the slip plane is not at the wall but in the vicinity of the wall and is called "strong". In this case the polymer-wall interactions are strong and the phenomenon of slip is effectively cohesive melt fracture. Both mechanisms should be possible when stress levels are high. In summary, little or no slip is observed at low shear rates, weak slip is observed at intermediate shear rates, and dramatic cohesive slip is evident at higher shear rates. Strong slip may show shear banding in which a slip plane characterized by a locally higher shear rate separates regions (bands) that are sheared at lower rates [10-12]. Experiments show that it is possible to reduce slip by changing the materials of construction of the wall or by adding a lubricious coating [13-16]. Controlling slip phenomena is of critical industrial importance in the processing of polymers at economically competitive rates [1, 3].

Khare et. al.,[17] Sun and Ebner,[18] Jabbarzadeh et. al.,[19, 20] and Priezjev and Troian[21] as well as Zhou et.al., [22] use Molecular Dynamics (MD) simulations to study slip phenomena. Khare et. al. are the first to show with MD simulations that polymeric fluids subject to shear flow experience a high degree of slip at the walls. Sun and Ebner show that slip depends on the energetic interactions of the polymer with the moving wall. Jabbarzadeh et. al. show slip for hexadecane and investigate the effect of wall features on the magnitude of slip. These authors found no evidence for strong slip but are able to observe and characterize weak slip. The most important factor was found to be the polymer-to-wall attractive interactions. Priezjev and Troian[21] demonstrate slip for unentangled coarse grained chains. These authors find a difference between the velocity of the molecules at the wall and the wall itself and were able to quantify a degree of weak slip. Many MD simulations of slip suffer from the limitation of being conducted at artificially low densities [23, 24]. However, a more recent study works at higher densities and finds highly nonlinear velocity profiles close to the interface and a nonlinear shear rate dependency for the slip length for unentangled chains[25]. More importantly, the shear rates that must be utilized in MD simulations are artificially high, on the order of 10^{10} up to 10^{13} s^{-1}! Such high shear rates are not representative of experiments; at normally accessible experimental rates small molecules and short (unentangled) polymers show little evidence of slip. The study by Zhou[22] is an exception – a coarse grained MD model of polycarbonate melt is performed at shear rates on the order of 10^5 s^{-1}. Chains with two strongly adsorbing end groups are observed to slip relative to the wall (adhesive slip) and the bulk chains are also observed to slip relative to the adsorbed layer (strong slip). Despite the lower shear rates of the study and a follow on study [26]the chains are observed to always slip. Only upon the addition of a low molecular weight additive is a no-slip boundary condition observed at the lowest shear rates studied. So despite the progress made in understanding slip phenomena there are still questions that have not been fully answered, *particularly for high molecular weight materials* where conventional simulation techniques remain computationally prohibitive. In a recent review by Hazikirakos[2] the effects of molecular characteristics, such as long chain branching and polydispersity, on slip effects is noted as being poorly understood.

In the present work, flowing polymer chains between neutral walls (that is "hard" walls in which the attractive interactions between polymer segments and the wall are taken to be zero) are studied using a biased Dynamic Monte Carlo (DMC) algorithm [27-29]. This coarse grained lattice model combines cooperative motion with flow in an algorithm known as COMOFLO. Under quiescent conditions, it properly reproduces Rouse and reptation dynamics as measured through characteristic correlation functions. When biased to model flow, detailed balance is not obeyed and viscous heating effects are not captured; there are no temperature variations present in the present simulations.

Here the COMOFLO algorithm is applied to understanding slip in plane parallel shear flow. The stress tensor is calculated using Kramer's bead-spring treatment[30, 31] from the dyadic product of the bond orientation vectors, $\underline{r}$, according to $\underline{\underline{\sigma}}=2\nu kT\beta^2\langle \underline{r}\,\underline{r}\rangle$ where ν is the number of chains per unit volume and β is defined as $3/(2Nl^2)$. N is the number of chain segments and l is the length of a Kuhn segment. The total dimensionless stress tensor is given by Equation 1.

$$\frac{\underline{\underline{\sigma}}}{2\nu kT}=\frac{3\langle \underline{r}\,\underline{r}\rangle}{2Nl^2}=\frac{3\langle \underline{r}\,\underline{r}\rangle}{2\langle R^2\rangle} \qquad (1)$$

where $\langle R\rangle^2$ is the mean-squared end-to-end vector under unperturbed and unconfined conditions. For the present model, $\langle R^2\rangle^{1/2}=1.58N^{0.5}$ [32]. The deviatoric stress tensor, $\underline{\underline{\tau}}$, is calculated by subtracting the static stress tensor (calculated from Equation 1 under quiescent conditions) from the total stress tensor. One unit of Monte Carlo time (mct) is defined as when the number of Monte Carlo moves is equal to the total number of segments (monomers) in the simulation box. [33] Velocity is calculated by monitoring the displacement of the segments (measured in Monte Carlo (i.e. lattice) sites (mcs)) as a function of Monte Carlo time. The apparent shear rate, $\dot{\gamma}_a$, is calculated by fitting a linear function to the velocity versus plate spacing data. In the simulations presented here, plate spacing is set at approximately ten times the unconfined and unperturbed radius of gyration for each chain length studied; in presenting the results all plate spacings are normalized to a quantity L* ranging from 0 to 1. Non-periodic dimensions exceed two times the maximum magnitude of the end-to-end chain vector in order to satisfy the minimum image convention. Further details of the COMOFLO simulation technique can be found in Dorgan et. al. [27]

Mapping of the lattice model on to real chains is of interest to assess the physical reality of the simulations. Associating the lattice segment with an ethylene group of polyethylene, a comparison of the end-to-end vector yields a value of $3.65\dot{A}$; if the experimental melt density (0.866 g/cm^3 at 140 °C) is used, the value is $3.77\dot{A}$. Adopting a value of $3.7\dot{A}$, comparison of the mean-squared displacement of the center of mass motion against experimental values[34] yields a value of 1.0×10^{-11} (s/mct). Accordingly, simulation shear rates from the lowest of 10^{-7} (1/mct) to the highest of 10^{-3} (1/mct) correspond to physical shear rates from 10^4-10^8 s^{-1}. The ability to access these lower shear rates enables observation of all regimes in the no-slip to strong slip cascade.

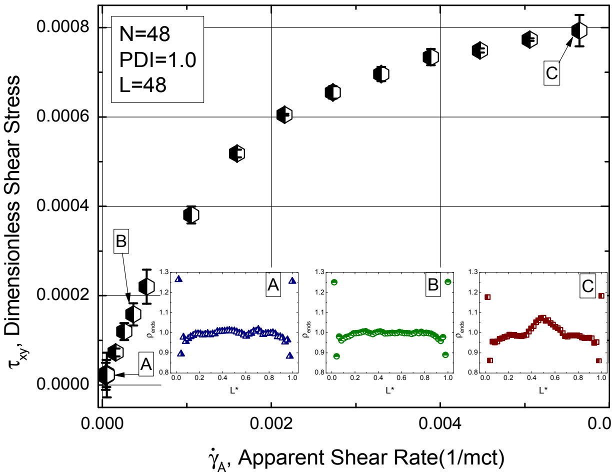

Figure 1. Shear stress vs. shear rate for *unentangled monodisperse chains* having N=48 segments; the inset shows chain end distributions across the plate spacing. At high shear rates evidence of cohesive failure (strong slip) is evident in the chain end distribution at point C.

Slip can be observed by examining the stress response and velocity profiles. Figure 1 shows the calculated stress response for an unentangled system which exhibits Rouse dynamics under quiescent conditions. These unentangled chains show non-Newtonian behavior; a shear thinning viscosity is clearly present. Importantly, the stress is monotonic with increasing shear rate and remains so for all achievable rates. Figure 1 also shows the chain end density for low, moderate, and high shear rates. Chain end density, ρ_{ends}, is defined as the number of chain ends in a given plane parallel to the walls divided by the number of chain ends under the assumption of equal distribution throughout the box. At low and moderate shear rates chain ends are in slight excess at the walls, have a slight depletion in the layers near the wall, and approach uniformity in the middle of the gap. Despite the stress response being monotonic, at high enough shear rates the chain end density shows evidence for cohesive failure, or strong slip. An excess of chain ends develops at the mid-plane indicating segregation and slipping.

Figure 2 shows the corresponding velocity profiles for different shear rates for the unentangled case. At low and moderate shear rates, a linear velocity profile is obtained. Importantly, for all shear rates there is no evidence of slip at the wall; "weak" slip for unentangled chains is not observed.

Without entanglements the flowing chains cannot exert stresses high enough to make the adsorbed chains slip relative to the wall. This is consistent with experimental findings [2, 3, 9, 10] but distinct from MD simulations performed at unrealistically high shear rates [17-21]. As the simulations are extended to higher shear rates evidence for cohesive failure manifests itself in the velocity profile. Cohesive slip is observable as a region of higher shear rate (a steeper velocity profile) in the middle of the simulation box. This region of higher shear rate corresponds to the region in which there is an excess of chain ends as seen in Figure 1. The finding of cohesive slip at very high shear rates is consistent with careful independent examination of the velocity profiles reported in earlier MD studies even though these small anomalies in the velocity profiles were not explicitly acknowledged by the presenting investigators. [19-21]

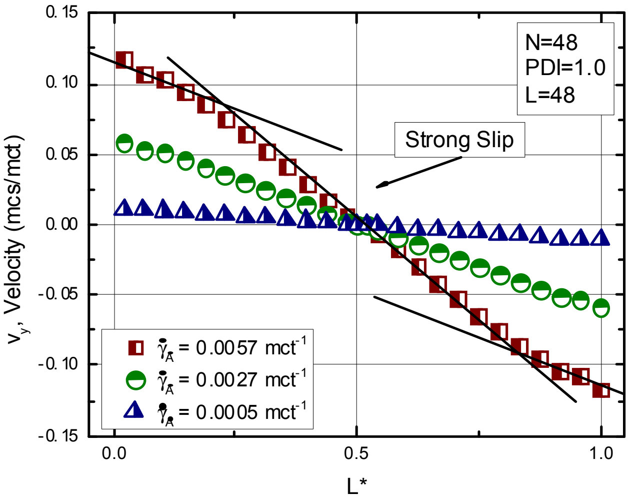

Figure 2. Velocity profiles for different apparent shear rates corresponding with the data of Figure 1. These lower molecular weight chains show no evidence of weak slip at the wall (adhesive failure) but do show strong slip (cohesive failure) at sufficiently high shear rates.

Figure 3 presents the shear stress as a function of shear rate for monodisperse *entangled* polymers. Strikingly, as shear rate increases a critical stress is reached after which the stress responses becomes non-monotonic. This implies there is an inherent rheological instability or bifurcation in which the same stress level could be supported by two different shear rates. This finding is consistent with observations of so-called "stick-slip" textures sometimes observed when processing polymers at high rates [1, 3]. At higher shear rates the polymers exhibit a cohesive failure; this failure is seen in the large excess of chain ends in the center of the box. Unlike the unentangled polymers, the entangled polymers show pretransitional stacking in the chain end density leading up to the bifurcation in the stress responses. Pretransitional phenomena have been observed in experiments on wall slip [11-13, 35-37].

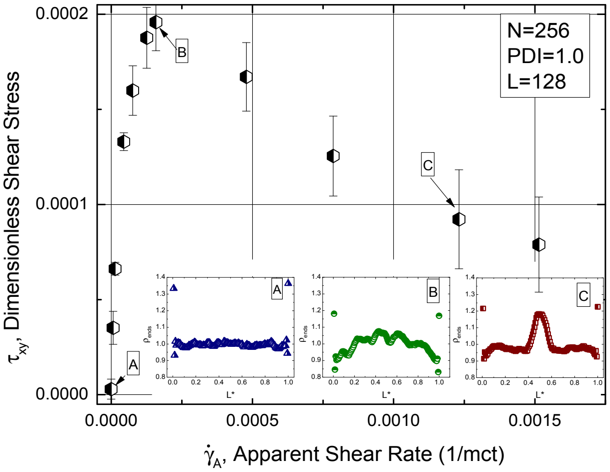

Figure 3. Shear stress vs. apparent shear rate for *entangled monodisperse chains* having N=256 segments. The stress response is non-monotonic implying inherent rheological instability. Strong cohesive failure is evident in the chain end distribution at high shear rates. Also, pretransitional "stacking" in the chain end distribution is evident at point B, the point of incipient instability.

Figure 4 presents the velocity profiles corresponding to the stresses presented in Figure 3. At low shear rates there is no evidence of slip but at intermediate shear rates the weak slip phenomena described above is observed. Ultimately, at the highest shear rates there is clear evidence of both weak slip near the wall and strong slip in the bulk. Near the mid-plane, corresponding to the region of excess chain ends, there is a region of high shear rate; shear banding is clearly present.

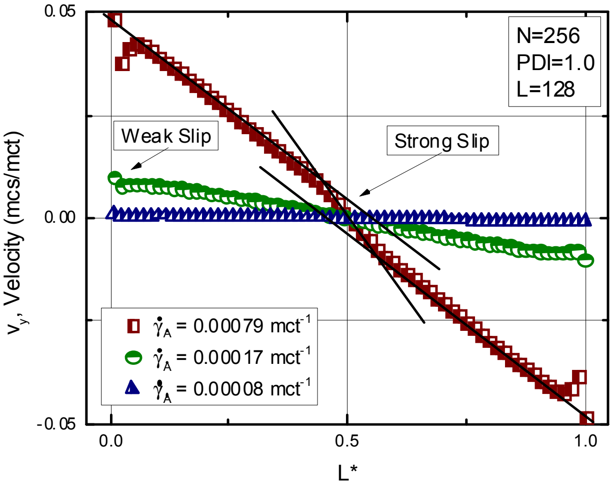

Figure 4. Velocity profiles for different apparent shear rates corresponding with the data of Figure 3. These higher molecular weight monodisperse chains show weak slip at the wall (adhesive failure) near the point of insipient instability and both weak and strong slip (cohesive failure) at sufficiently high shear rates.

The simulations also support the hypothesized coil-stretch [8, 10] transition for entangled polymers. At low and moderate shear rates the root mean squared end-to-end vector within one radius of gyration of the walls increases rapidly by about 30% – the quiescent "coil" becomes "stretched". At the maximum stress level cohesive failure occurs and the magnitude of the vector then increases in a nearly linear manner. For the unentangled polymers, the end-to-end vector scales linearly for all shear rates. Accordingly, these findings support the coil-stretch transition and loss of entanglements first proposed by Brochard and deGennes [8]. However, this mechanism is profoundly exaggerated by the monodisperse nature of the ensemble of chains.

Experimental findings have shown that it is possible to reduce the degree of instability by incorporating greater polydispersity in the polymers being processed. Figure 5 presents the calculated stress as function of apparent shear rate for a system of linear polymers with an average length of 256 but a a polydispersity index of 3.2. While the polydispersity index is moderately high, the system is composed of only five discreet chain lengths (N=64, 128, 256, 512, and 1024). This polymer system also demonstrates reptation dynamics under quiescent conditions. In strong contrast to the monodisperse case, the polydisperse shear stress vs. shear rate response is nearly monotonic. Only a small region in the curve exists where rheological instability would occur due to a stress bifurcation. The overall shape of this stress response curve, including the slight bifurcation, is reported in a number of experiments [2, 38, 39]. At low shear rates the chain ends are fairly evenly distributed throughout the box. It is noteworthy that in this polydisperse case there are more total chain ends than in the analogous monodisperse case of Figures 3 and 4 (2048 total chain ends for PDI =1 and 6662 chain ends for PDI=3.2). As shear rate increases the shorter chains preferentially move to the middle of the simulation box (as the system is athermal, this is an entropically driven effect) and thus the density of chain ends increases in the middle of the box. At high shear there is only a moderate excess of chain ends in the middle of the box. The effect of polydispersity is to create a more uniform distribution of chain ends across the gap width.

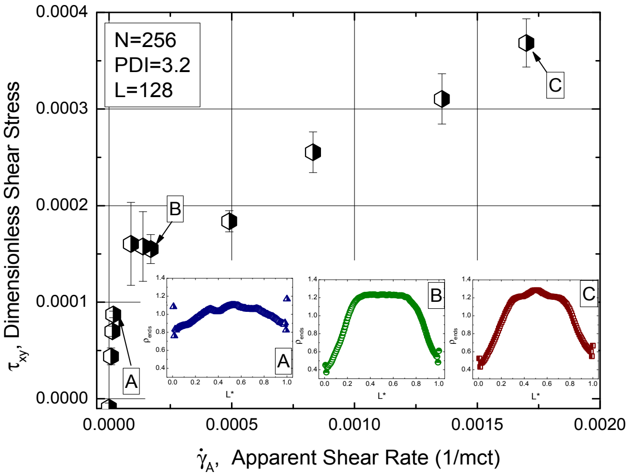

Figure 5. Shear stress vs. apparent shear rate for *entangled polydisperse chains* having N=256 segments; the inset shows chain end distributions across the plate spacing. The stress response is nearly monotonic implying only a very small region of inherent rheological instability. Little cohesive failure is evident in the chain end distribution at high shear rates.

The suppression of slip is also seen in the corresponding velocity profiles of Figure 6. Weak slip is still observed for moderate shear rates at the wall; however at high shear rates the region over which strong slip occurs is broadened in comparison to the monodisperse case.

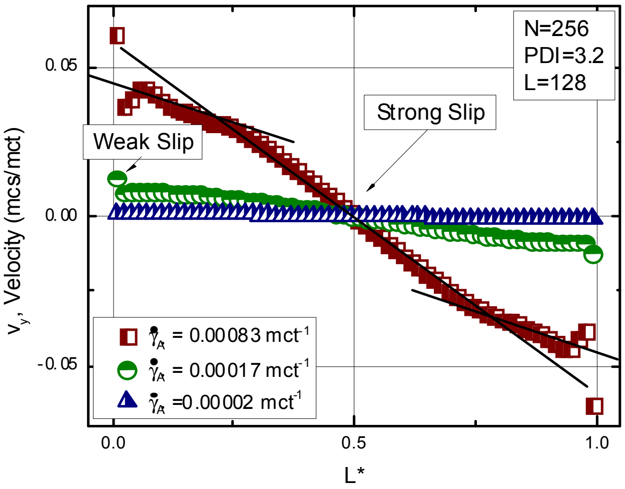

Figure 6. Velocity profiles for different apparent shear rates corresponding with the data of Figure 3. These higher molecular weight polydisperse chains show weak slip at the wall (adhesive failure) and both weak and strong slip (cohesive failure) at sufficiently high shear rates. However the region over which strong slip occurs is broadened compared to the monodisperse case.

Conclusions:

New molecular scale details regarding the phenomena of polymer wall slip are available through the use of a coarse grained dynamic Monte Carlo technique. The COMOFLO algorithm combines cooperative movement with field biasing to simulate polymer flow. Results for basic rheological properties[27] and the results of this study on wall-slip phenomena are in agreement with experiments[2, 3, 9, 10] and some elements of MD studies. [17-21]

Polymers having lengths well below the critical molecular weight for entanglement do not show evidence of slip until very high shear rates are reached. Even then, wall slip does not occur - only a strong slip phenomena involving cohesive failure of the unentangled melt is seen. Fluid stresses are not large enough to overcome polymer-wall interactions. Monodisperse entangled chains exhibit both weak (adhesive) and strong (cohesive) slip phenomena. Disentanglement is clearly evidenced in a non-linear velocity profile that exhibits shear banding, in an excess of chain ends at the slip plane, and in a non-monotonic stress vs. shear rate response. Direct evidence for the coil-stretch transition and loss of entanglement is present. Even moderate polydispersity severely reduces slip phenomena broadening the region of cohesive slip and leading to a more even distribution of chain ends.

The first molecular scale simulation of polydisperse entangled polymers exhibiting slip demonstrates the complexity of the issues involved in this long standing problem in fluid mechanics and suggests several areas of future investigation.

This work was funded by the Fluid Dynamics Program of the National Science Foundation under grant CBET-1067707.

REFERENCES:

[1] M. M. Denn, Annual Review of Fluid Mechanics 33 (2001).
[2] S. G. Hatzikiriakos, Progress in Polymer Science 37 (2012).
[3] L. Archer, in *Polymer Processing Instabilities: Control and Understanding*2005), pp. 73.
[4] E. Lunga, M. P. Brenner, and H. A. Stone, in *Handbook of Experimental Fluid Dynamics* (Springer, 2007).
[5] C. H. Choi and C. J. Kim, Physical Review Letters 96, 066001 (2006).
[6] C. L. H. M. Navier, Mem. Acad. Sci. Inst. Fr. 6 (1827).
[7] M. Mooney, Journal of Rheology 2 (1931).
[8] F. Brochard and P. G. Degennes, Langmuir 8 (1992).
[9] V. Mhetar and L. A. Archer, Macromolecules 31 (1998).
[10] S. Q. Wang, Polymers in Confined Environments 138 (1999).
[11] P. D. Olmsted, Rheologica Acta 47 (2008).
[12] F. J. Lim and W. R. Schowalter, Journal of Rheology 33 (1989).
[13] S. Q. Wang and P. Drda, Macromol. Chem. Phys. 198 (1997).
[14] S. G. Hatzikiriakos, C. W. Stewart, and J. M. Dealy, International Polymer Processing 8 (1993).
[15] S. G. Hatzikiriakos and J. M. Dealy, International Polymer Processing 8 (1993).
[16] S. G. Hatzikiriakos, International Polymer Processing 8 (1993).
[17] R. Khare, J. J. dePablo, and A. Yethiraj, Macromolecules 29 (1996).
[18] M. Sun and C. Ebner, Physical Review Letters 69 (1992).
[19] A. Jabbarzadeh, J. D. Atkinson, and R. I. Tanner, Physical Review E 61 (2000).
[20] A. Jabbarzadeh, J. D. Atkinson, and R. I. Tanner, Journal of Chemical Physics 110 (1999).
[21] N. V. Priezjev and S. M. Troian, Physical Review Letters 92, 018302 (2004).
[22] X. Zhou, D. Andrienko, L. D. Site, and K. Kremer, EPL (Europhysics Letters) 70 (2005).
[23] M. Sun and C. Ebner, Physical Review A 46 (1992).
[24] D. K. Bhattacharya and G. C. Lie, Physical Review A 43 (1991).
[25] A. Niavarani and N. V. Priezjev, Physical Review E 77 (2008).
[26] X. Zhou, D. Andrienko, L. D. Site, and K. Kremer, The Journal of Chemical Physics 123 (2005).
[27] J. R. Dorgan, N. A. Rorrer, and C. M. Maupin, Macromolecules 45 (2012).
[28] S. S. Gleiman and J. R. Dorgan, Journal of Chemical Physics 112 (2000).
[29] T. Pakula, in *Simulation Methods for Polymers*, edited by M. Kotelyanskii, and D. N. Theodorou (Marcel Dekker, New York, NY, 2004), pp. 147.
[30] H. A. Kramers, Journal of Chemical Physics 14 (1946).
[31] R. G. Larson, *Constitutive Equations for Polymer Melts and Solutions* (Butterworth-Heinemann, Butterworths, New York, 1988).
[32] R. S. PaiPanandiker, J. R. Dorgan, and T. Pakula, Macromolecules 30 (1997).
[33] K. F. Mansfield and D. N. Theodorou, Macromolecules 22 (1989).
[34] H. Tao, T. P. Lodge, and E. D. von Meerwall, Macromolecules 33 (2000).
[35] S. Q. Wang, P. A. Drda, and Y. W. Inn, Journal of Rheology 40 (1996).
[36] S. G. Hatzikiriakos and J. M. Dealy, Journal of Rheology 35 (1991).
[37] S. G. Hatzikiriakos and J. M. Dealy, Journal of Rheology 36 (1992).
[38] M. Ansari, S. G. Hatzikiriakos, A. M. Sukhadia, and D. C. Rohlfing, Polymer Engineering and Science 52 (2012).
[39] Y. H. Lin, Journal of Rheology 29 (1985).